ELSEVIER

Journal of Molecular Catalysis A: Chemical 188 (2002) 189–200

JOURNAL OF MOLECULAR CATALYSIS A: CHEMICAL

www.elsevier.com/locate/molcata

Manganese-containing MCM-41 for epoxidation of styrene and stilbene

Qinghong Zhang [a], Ye Wang [b], Satoko Itsuki [a], Tetsuya Shishido [a], Katsuomi Takehira [a,*]

[a] *Department of Applied Chemistry, Graduate School of Engineering, Hiroshima University, Kagamiyama 1-4-1, Higashi-hiroshima 739-8527, Japan*

[b] *State Key Laboratory for Physical Chemistry of Solid Surfaces, Department of Chemistry, Xiamen University, Xiamen 361005, China*

Received 22 November 2001; received in revised form 2 May 2002; accepted 15 May 2002

Abstract

Mn-MCM-41 is found to be the most effective heterogeneous catalyst for the epoxidation of styrene with *tert*-butyl hydroperoxide (TBHP) among several metal ion-containing mesoporous molecular sieves including Mn-, V-, Cr-, Fe-, and Mo-MCM-41. ESR, XANES, diffuse reflectance UV–VIS, UV–Raman and XPS are used to characterize the Mn-MCM-41 synthesized by both direct hydrothermal (DHT) and template ion exchange (TIE) methods. The results suggest that Mn^{2+} and Mn^{3+} coexist in the Mn-MCM-41 samples synthesized by both methods and a large part of manganese atoms could be incorporated into the framework of MCM-41 obtained by the DHT method. The oxidation of either styrene or stilbene with TBHP as the oxidant over the Mn-MCM-41 produces corresponding epoxide as the main product; the reaction probably proceeds through a radical intermediate. The TIE catalyst shows higher activity, while the DHT catalyst gives higher TBHP efficiency for the epoxidation reactions.

Keywords: Mn-MCM-41; Epoxidation; *tert*-Butyl hydroperoxide; Styrene; Stilbene

1. Introduction

Since MCM-41 possesses large surface area ($\sim$1000 $m^2\,g^{-1}$) and uniform mesopore with controllable diameter of 2–10 nm, it is expected as a desirable material for catalytic applications. However, in most cases, siliceous mesoporous materials do not have sufficient intrinsic activities as catalysts, and thus many studies have concentrated on introducing catalytically active sites such as metals, metal ions and metal complexes into mesoporous silica [1,2]. The most popular method for the introduction of active sites is the direct hydrothermal (DHT) method, i.e. direct addition of the metal ion precursors to the synthesis gel before hydrothermal synthesis. The conventional impregnation method has also been used to deposit active component onto MCM-41; however this method cannot ensure the incorporation of active species into the mesopore of MCM-41, and some contractions of channels seem to occur during wet impregnation [3]. Several groups reported grafting methods [4–6], i.e. grafting of organometallic complexes or metal ions onto the surface of mesoporous silica by using surface silanol groups as anchor sites. Metal ions can also be implanted into MCM-41 with the template ion exchange (TIE) method [7], i.e. by

* Corresponding author. Tel.: +81-824-24-7744; fax: +81-824-22-7191.
E-mail address: takehira@hiroshima-u.ac.jp (K. Takehira).

1381-1169/02/$ – see front matter
PII: S1381-1169(02)00323-0

exchanging the template cations embraced in the channels of the as-synthesized MCM-41 with the metal ions in solution.

It can be expected that different synthetic methods would result in different environments of the active sites introduced to MCM-41. Oldroyd et al. [8] reported that Ti-MCM-41 prepared by surface grafting method was more active than that prepared by the DHT method for the epoxidation of cyclohexene with TBHP. We have shown that V-MCM-41 prepared by the TIE and DHT methods possesses different coordination environment of vanadium and behaves differently in the partial oxidation of lower alkanes [9–11]. Vanadium species introduced by the TIE method are mainly dispersed on the surface of channel, preferring the oxidative dehydrogenation of ethane and propane, whereas vanadium sites introduced by the DHT method are mainly incorporated inside the framework of MCM-41, capable of oxidizing propane to acrolein with moderate selectivity. Recently, we found that Fe-MCM-41 prepared by the TIE and DHT methods showed remarkably different coordination environment of iron, resulting in different catalytic performance for epoxidation of styrene with H_2O_2 [12].

Manganese complexes are well known catalysts for epoxidation reactions [13]. Recently, many research groups worked on the immobilization of Mn complexes onto the mesoporous material. Although ion-exchange method was applied to Al-MCM-41 [14], only lower loading amount can be obtained by this method. Caps and Tsang [15] prepared Mn-MCM-41 with a molecular organic chemical vapor deposition (MOCVD) method. Burch et al. [16] prepared surface-grafted manganese-oxo species on the walls of MCM-41 channels and applied it for the complete oxidation of propene. Iwamoto and coworkers [7] firstly developed the TIE method for the synthesis of Mn-MCM-41, and they argued that manganese was highly dispersed in the mesopore of MCM-41 and only existed as Mn^{2+}. The Mn-MCM-41 thus prepared exhibited high activity for the epoxidation of stilbene with TBHP [17].

In the present paper, several metal ion-containing mesoporous molecular sieves including Mn-, V-, Cr-, Fe- and Mo-MCM-41 are screened for the epoxidation of styrene using TBHP as an oxidant. With the most effective Mn-MCM-41, the influences of synthetic methods (the DHT and TIE methods) on the nature of manganese species and catalytic properties in the epoxidation of either styrene or stilbene are subsequently investigated.

2. Experimental

2.1. Catalyst preparation

MCM-41 was prepared by hydrothermal synthesis at 120 °C for 96 h using sodium silicate and hexadecyltrimethylammonium bromide ($C_{16}H_{33}(CH_3)_3NBr$) as the silicon source and the template, respectively. For the TIE synthesis of Mn-MCM-41, 2 g of the as-synthesized MCM-41 containing ca. 50 wt.% template cations was added to an aqueous solution of manganese(II) nitrate (e.g. 48.7 mg $Mn(NO_3)_2{\cdot}6H_2O$ in 40 ml of H_2O for the preparation of the Mn-MCM-41, TIE, Si/Mn = 124). The mixture was stirred vigorously at ambient temperature for 1 h, and then kept at 80 °C for 20 h. The as-synthesized Mn-MCM-41 (TIE) was finally calcined by heating to 550 °C at a rate of 1 °C min^{-1} and kept at 550 °C for 6 h in a flow of dry air (1 dm^3 min^{-1}). For the DHT synthesis of Mn-MCM-41, the solution of manganese nitrate was added to the mixture of sodium silicate and $C_{16}H_{33}(CH_3)_3NBr$. For the synthesis of the Mn-MCM41 (DHT, Si/Mn = 91), 41.7 mg $Mn(NO_3)_2{\cdot}6H_2O$ was added to the mixture of 15.4 g of sodium silicate and 26.4 g of $C_{16}H_{33}(CH_3)_3NBr$ in 350 ml H_2O. After hydrothermal synthesis at 120 °C for 96 h, the product was filtered, washed thoroughly with deionized water, dried at 40 °C in vacuum for 24 h and finally calcined by the same procedure as described for the TIE method.

Vanadium, chromium and iron were also introduced to MCM-41 by the DHT method following the same procedure described above using VOC_2O_4, $Cr(NO_3)_3{\cdot}9H_2O$ and $Fe(NO_3)_3{\cdot}9H_2O$ as the sources of V, Cr, and Fe respectively. Molybdenum was introduced by the TIE method using MoO_2-AA (bis(2,4-pentanedionato)molybdenum dioxide(II)) as the source of Mo.

2.2. Catalyst characterization

X-ray diffraction (XRD) patterns were recorded with an SRA M18XHF diffractometer using Cu Kα

radiation (40 kV, 300 mA). Small divergent and scattering slits (0.05 and 0.05 mm) were used to avoid the high background radiation at low diffraction angle. N_2 adsorption isotherms at 77 K were measured using a BELSORP 18SP apparatus (volumetric), and pore size distribution was obtained by the Dollimore and Heal (DH) method [18]. The content of manganese in each sample was determined by ICP measurement using a Perkin-Elmer OPTIMA 3000.

ESR spectroscopic measurements were carried out at X-band (∼9 GHz) using a JEOL RE series JES-RE1X ESR spectrometer. The powdery sample was loaded into a quartz tube with inner diameter of 3 mm and measured at ambient temperature. X-ray absorption experiments were carried out at Photon Factory in National Laboratory for High Energy Physics (KEK-PF), Tsukuba, Japan, on the BL7C station with apparatus operated in the fluorescence and transmission modes with a doublecrystal Si (1 1 1) monochrometer. Ring energy and ring current were 2.5 GeV and about 350–380 mA, respectively. Energy was calibrated with Mn K-edge absorption of Mn foil (6538.0 eV). Energy step of measurement in XANES region was 0.3 eV.

The diffuse reflectance UV–VIS spectra were recorded on a Perkin-Elmer UV–VIS–NIR spectrometer (Lambda 900). The powder was loaded in a quartz cell, and the spectra were collected between 200 and 700 nm referenced to $BaSO_4$. UV–Raman measurements were carried out using a Renishaw UV–VIS Raman System 1000R. The UV line at 325 nm from a Kimmon IK3201R-F He–Cd laser was used as the exciting source. A laser output of 30 mW was used and the maximum incident power at the sample was approximately 6 mW. XPS measurements were performed on a Shimadzu ESCA-85 spectrometer working with a hemispherical analyzer. All binding energy values were referenced to C 1s (284.6 eV).

2.3. Catalytic reaction

Styrene (>98%), *trans*-stilbene (>98%), *tert*-butyl hydroperoxide (TBHP) (70% aqueous solution) (Wako Pure Chemical Industries) and *cis*-stilbene (>95%) (Tokyo Kasei) were used as reactants without further purification. Catalytic reactions were carried out according to the following procedure. Substrate, solvent and catalyst were first introduced into a round-bottom flask. After oxidant was added, the reaction was started by immersing the flask into water bath kept at the reaction temperature. The reaction was carried out under violent stirring. All the products were quantified by a gas chromatograph (Shimadzu GC-14B) equipped with a BPX5 capillary column and an FID detector using toluene as an internal standard. *tert*-Butyl alcohol produced from TBHP was also analyzed, from which TBHP conversion was estimated. GC–MS (Shimadzu GCMS-QP5050A) and NMR (JEOL FT-NMR Lambda 400NMR) were also used to identify the products.

3. Results and discussion

3.1. Epoxidation of styrene over several metal ion-containing MCM-41

Table 1 shows the catalytic results of several metal ion-containing MCM-41 in the epoxidation of styrene using TBHP as an oxidant. It should be noted that XRD measurements of all these samples showed four diffraction lines at 2θ degrees of 2–6° ascribed to the (1 0 0), (1 1 0), (2 0 0) and (2 1 0) of MCM-41, suggesting that the mesoporous structure was retained after the introduction of each metal ion. The oxidation of styrene gave two main products, i.e. styrene oxide and benzaldehyde (abbreviated as Sty.oxide and Benzald., respectively in Tables 1, 4 and 5), and TBHP was converted into *tert*-butyl alcohol. The efficiency of TBHP was evaluated from the amount of the oxidative products produced from styrene divided by the amount of the TBHP consumed. In the absence of catalyst, the yield of styrene oxide was 2.9% at 60 °C. Pure siliceous MCM-41 gave a yield of styrene oxide of 6.2%. Although V-MCM-41 exhibited the highest styrene conversion of 20% with a 74.6% selectivity of styrene oxide, a serious leaching of V species was observed, resulting in the complete deactivation when the recovered catalyst was used in the second run. The leaching of Cr also took place, and the color of Cr-MCM-41 changed from orange to white after the reaction. The conversions of styrene over Fe- and Mo-MCM-41 were lower than that of pure silicious MCM-41. Among the tested samples, Mn-MCM-41 showed no leaching and gave the highest selectivity to styrene oxide (81.9%) as well as the highest TBHP

Table 1
Oxidation of styrene using TBHP as oxidant over several metal ion-containing MCM-41[a]

Catalyst (Si/M)	Styrene conversion (%)	Selectivity (%)		Sty.oxide yield (%)	TBHP conversion (%)	TBHP efficiency (%)
		Sty.oxide	Benzald.			
Mn-MCM-41(47), DHT	17.9	81.9	18.0	14.6	18.0	100.0
V-MCM-41(24), DHT	20.1	74.6	25.4	15.0	33.9	59.0
Cr-MCM-41(50), DHT	9.7	68.4	31.6	6.6	20.4	47.5
Fe-MCM-41(25), DHT	5.2	47.9	52.1	2.5	11.6	44.8
Mo-MCM-41(32), TIE	5.7	53.8	46.2	3.1	9.3	61.3
MCM-41	8.9	65.9	30.6	6.2	10.0	89.0
Blank test	5.5	52.7	47.3	2.9	7.6	72.4

[a] Catalyst, 0.2 g; $T = 60\,^{\circ}C$; $t = 24$ h; DMF, 1 ml; MeCN, 9 ml; styrene, 10 mmol; TBHP, 10 mmol.

efficiency (100%). Thus, Mn-MCM-41 was the most effective heterogeneous catalyst for the epoxidation of styrene with TBHP as the oxidant.

Mn-MCM-41 prepared by the TIE method was reported to be effective for the epoxidation of stilbene in a previous study [17]. As described above, different synthetic methods would lead to active species with different nature and coordination environments. In our studies, we characterize the Mn species introduced into MCM-41 by both DHT and TIE methods in detail and compare their catalytic properties in the epoxidation of both styrene and stilbene.

3.2. Structure of Mn-MCM-41

XRD patterns of Mn-MCM-41 with different Si/Mn ratios synthesized by both DHT and TIE methods are shown in Fig. 1. In a similar manner to the results reported in [7], the TIE samples exhibited four typical diffraction peaks assigned to the (1 0 0), (1 1 0), (2 0 0) and (2 1 0) reflections of a regular hexagonal array of channels of MCM-41 (Fig. 1d–f). The intensity of each peak did not significantly change with increasing Mn content to 1.48 wt.% (Si/Mn = 61), indicating no deorganization at long range of the mesoporous structure of MCM-41 during the TIE synthesis. On the other hand, the DHT samples showed a clear decrease in the peak intensity with an increase in Mn content (Fig. 1a–c). A similar phenomenon was also observed when other metal cations were introduced into MCM-41 by using the DHT method, and was suggested to relate with the existence of non-silica component in the wall of MCM-41 [19]. When the Mn content increased to 1.91 wt.% (Si/Mn = 47), peak intensity was substantially weakened, indicating a serious decrease in the structural regularity. Concerning the peak position after introducing manganese, no clear shift was observed with an increase in Mn content. It should be noted that no Mn oxide phases were detected on the Mn-MCM-41 prepared by both TIE and DHT methods from the XRD measurements in high diffraction angle region and that the samples were pale pink in color. Thus, manganese

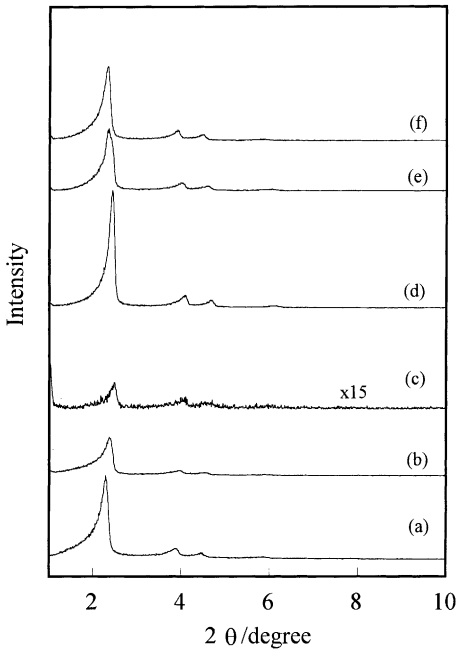

Fig. 1. XRD patterns of the Mn-MCM-41: (a) DHT, Si/Mn = 359; (b) DHT, Si/Mn = 91; (c) DHT, Si/Mn = 47; (d) TIE, Si/Mn = 214; (e) TIE, Si/Mn = 124; (f) TIE, Si/Mn = 61.

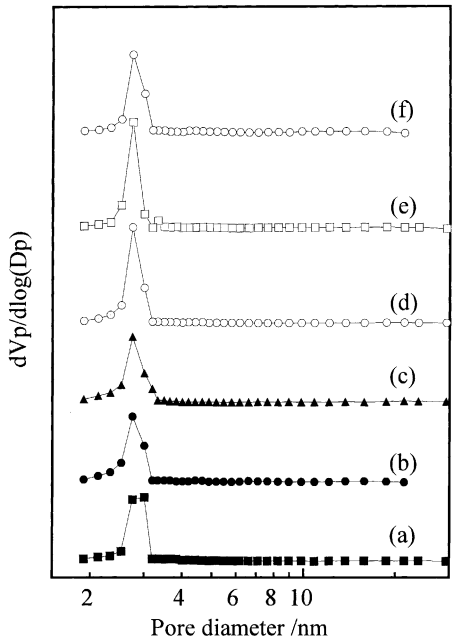

Fig. 2. Pore size distributions of the Mn-MCM-41: (a) DHT, Si/Mn = 359; (b) DHT, Si/Mn = 91; (c) DHT, Si/Mn = 47; (d) TIE, Si/Mn = 214; (e) TIE, Si/Mn = 124; (f) TIE, Si/Mn = 61.

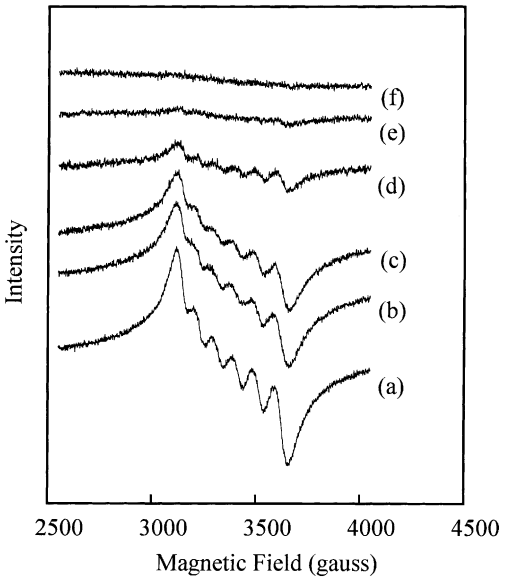

Fig. 3. ESR spectra of the Mn-MCM-41: (a) TIE, Si/Mn = 214; (b) TIE, Si/Mn = 124; (c) TIE, Si/Mn = 61; (d) DHT, Si/Mn = 359; (e) DHT, Si/Mn = 211; (f) DHT, Si/Mn = 47.

species were highly dispersed in the samples prepared by both methods.

Pore size distributions evaluated by N_2 adsorption isotherms using the DH method are shown in Fig. 2. Both the TIE samples (Fig. 2d–f) and the DHT samples (Fig. 2a–c) exhibited sharp pore size distributions around 2.7 nm. Porous properties of these samples are listed in Table 2. The surface area and pore volume slightly decreased with an increase in Mn content in both the cases.

ESR spectroscopy was employed to survey the oxidation states of Mn species introduced to MCM-41. Iwamoto and coworkers [7] found a typical Mn^{2+} ESR signal for the Mn-MCM-41 (Si/Mn = 20, TIE) and suggested that manganese existed as Mn^{2+} in their TIE sample. We compared the room temperature X-band ESR spectra of the TIE and DHT samples with various Si/Mn ratios in Fig. 3. All the Mn-MCM-41 samples

Table 2
Physical properties of Mn-MCM-41 prepared by the DHT and TIE methods

Si/Mn[a]	Method for synthesis	Si/Mn[b]	Mn content (wt.%)	Surface area[c] ($m^2\ g^{-1}$)	Pore volume[d] ($cm^3\ g^{-1}$)	Pore diameter[d] (nm)
200	TIE	214	0.43	1034	0.93	2.7
100	TIE	124	0.73	994	0.96	2.7
50	TIE	61	1.48	870	0.89	2.7
25	TIE	33	2.70	791	0.82	2.7
400	DHT	359	0.25	904	0.85	3.0
100	DHT	91	0.99	893	0.77	2.7
50	DHT	47	1.91	908	0.82	2.7

[a] Atomic ratios used in synthesis gel.
[b] Atomic ratios measured by ICP.
[c] Measured by the BET method.
[d] Evaluated from N_2 adsorption isotherms.

synthesized by the TIE method showed sextet lines with a g value of about 2 and a hyperfine coupling constant (A value) around 97 G, which were consistent with Mn^{2+} ($g = 2.0$, $A = 80$–100 G) in the environment of distorted octahedral symmetry. These values are also close to those reported for Mn-MCM-41 [20] and MnAPO-5 [21] with the Mn species located at extra-framework positions. The increase in Mn content broadened the hyperfine lines significantly and resulted in a considerable decrease in the resolutions of the whole spectra (Fig. 3a–c). This can be attributed to an increase in the spin exchange interaction due to a decrease in the Mn^{2+}–Mn^{2+} distance. For the DHT samples, only very weak sextet lines were observed even at very low Mn content (Fig. 3d–f). We think that this is probably due to the presence of Mn^{3+} species in the DHT samples, since Mn^{3+} is usually ESR silent owing to its large zero-field splitting [22]. The absence of any ESR signal for a Mn-containing mesoporous silica has been attributed to the presence of Mn(III) [23]. Since Mn^{3+} is more inclined than Mn^{2+} to be substituted for Si^{4+} at the framework position of zeolites or MCM-41, we speculate that a part of manganese ions may be incorporated inside the framework of MCM-41 as Mn^{3+} with the DHT method. The framework vanadium and iron species were mainly obtained respectively, when we introduced iron and vanadium into MCM-41 using the DHT method [11,12].

Table 3
X-ray absorption-edge positions for the catalysts and reference compounds

Sample	Edge position (eV)[a]
Mn-MCM-41, DHT (Si/Mn = 211)	6545.7
Mn-MCM-41, TIE (Si/Mn = 214)	6545.9
MnO	6542.9
Mn_3O_4	6545.9
Mn_2O_3	6548.1
MnO_2	6550.9

[a] Taken as the first major maximum in the derivative of the K-edge spectrum with respect to the corresponding feature of α-Mn metal (6538.0 eV).

The normalized Mn K-edge XANES spectra for both DHT and TIE samples as well as for the reference manganese oxides are shown in Fig. 4A, and the positions of the absorption edge are summarized in Table 3. The position of the absorption edge was taken as the first major peak in the corresponding derivative spectrum. As reported in [24–26], we have observed that the edge positions of the manganese oxides shift

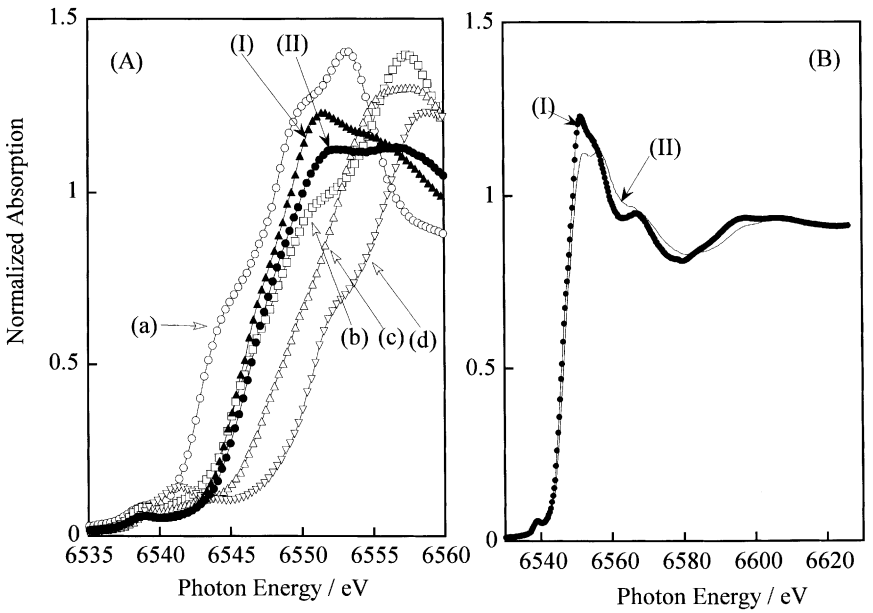

Fig. 4. Normalized Mn K-edge XANES spectra of the Mn-MCM-41 along with reference compounds. (I) Mn-MCM-41, DHT, Si/Mn = 211, (II) Mn-MCM-41, TIE, Si/Mn = 214. (a) MnO, (b) Mn_3O_4, (c) Mn_2O_3, (d) MnO_2.

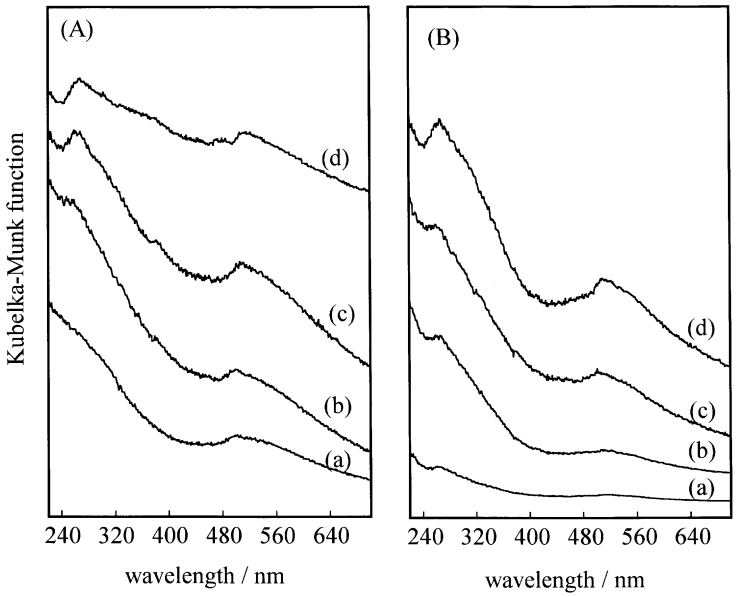

Fig. 5. Diffuse reflectance UV–VIS spectra of the Mn-MCM-41. (A) TIE samples, (a) Si/Mn = 214, (b) Si/Mn = 124, (c) Si/Mn = 61, (d) Si/Mn = 33; (B) DHT samples, (a) Si/Mn = 359, (b) Si/Mn = 211, (c) Si/Mn = 91, (d) Si/Mn = 47.

to high energy with an increase in the oxidation state ($MnO < Mn_3O_4 < Mn_2O_3 < MnO_2$). The edge positions of DHT and TIE samples were 6545.7 and 6545.9 eV, respectively. They were quite close to that of Mn_3O_4 (6545.9 eV), indicating the coexistence of Mn^{2+} and Mn^{3+} in both the samples. The shape of XANES spectrum for the DHT sample was, however, quite different from that of the TIE sample (Fig. 4B(I and II)). This indicates that the coordination environments of manganese in the two samples are different.

Fig. 5 shows the diffuse reflectance UV–VIS spectra of the Mn-MCM-41 synthesized by both the methods. Two bands at ca. 270 and 500 nm were observed for these samples. The $^6A_{1g} \rightarrow {}^4T_{2g}$ crystal field transitions of Mn^{2+} under the circumstance of Mn_3O_4 or MnO showed a band at 500 nm [27]. Thus, the band at 500 nm was assigned to Mn^{2+} probably existing on the surface of MCM-41. However, the band at 270 nm with such a high intensity was not reported in the literature. The charge transfer transition of $O^{2-} \rightarrow Mn^{3+}$ in Mn_3O_4 in which Mn was octahedronally coordinated with oxygen exhibited a band at ca. 320 nm [27,28]. We thus tentatively assigned the intense band observed at lower wavelength (270 nm) to the charge transfer transition of $O^{2-} \rightarrow Mn^{3+}$ in tetrahedral coordination, i.e. in the framework of MCM-41. At lower Mn content, mainly Mn^{2+} sites existed in the sample synthesized by the TIE method as shown in Fig. 5A(a and b), while the intensity of the band assigned to Mn^{2+} (500 nm) is relatively smaller and a larger number of Mn^{3+} sites exist in the DHT samples. These are consistent with those obtained from ESR measurements as described above. As Mn content increased, no obvious difference could be seen from UV–VIS spectra between these two types of samples, indicating that both types of Mn species coexist in the samples. It should be noted that the sensitivities of the bands at 270 and 500 nm may be different, and thus the intensities of these bands cannot be used to evaluate the ratios of Mn^{2+}/Mn^{3+} in the samples.

UV–Raman spectroscopy was used for the characterization of transition metal atoms such as Ti and V in the framework of molecular sieves [29–31]. Fig. 6 shows the UV–Raman spectra of Mn-MCM-41 synthesized by both DHT and TIE methods. Weak Raman bands at ca. 500 and 970 cm^{-1} were observed in the spectrum of pure silicious MCM-41. These bands can be assigned to symmetric stretching vibrations of the

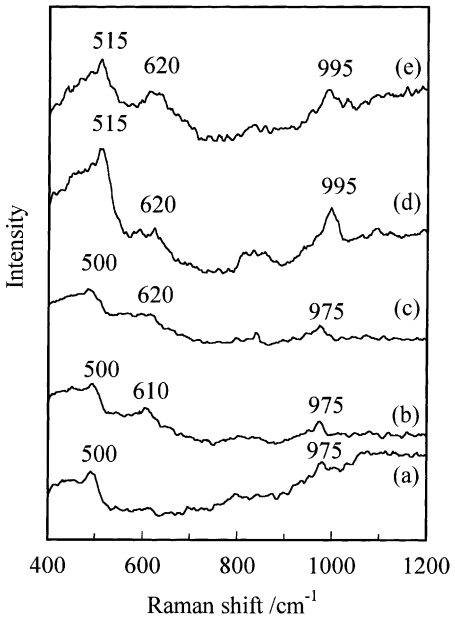

Fig. 6. UV–Raman spectra of the Mn-MCM-41: (a) MCM-41; (b) TIE, Si/Mn = 214; (c) Si/Mn = 124; (d) DHT, Si/Mn = 359; (e) DHT, Si/Mn = 211.

Si–O–Si and anti-symmetric stretching of the Si–O–Si vibrations in defects, e.g. the presence of OH connected to the adjacent Si, respectively [29,31]. A very weak Raman band at 610–620 cm^{-1} was newly observed for the Mn-MCM-41 synthesized by the TIE method. This band was more distinct and other two additional bands at 515 and 995 cm^{-1} were observed more clearly for the DHT samples. These bands cannot be assigned to any bulk Mn oxide phases [33]. A band at 615 cm^{-1} close to that at 620 cm^{-1} observed here was reported in a Raman study of silica supported manganese oxide, and was considered as a vibration due to interface Mn–O–Si bonding [33]. We thus think that the band at 610–620 cm^{-1} can be ascribed to surface manganese species on MCM-41. Two bands at 520 and 1110 cm^{-1} were observed in the UV–Raman spectrum of Ti-MCM-41 and were assigned to the symmetric and asymmetric stretching vibrations of Si–O–Ti in the framework of MCM-41 [32]. Therefore, it is reasonable to ascribe the newly observed bands at 515 and 995 cm^{-1} in the spectra of Mn-MCM-41 synthesized by the DHT method to the symmetric and asymmetric stretching vibrations of Si–O–Mn in the framework of MCM-41. These two bands did not increase with an increase in Mn content, probably suggesting that the amount of Mn existing in the framework of MCM-41 was very limited. The results obtained from UV–Raman studies further suggest that a part of manganese ions can be incorporated into the framework of MCM-41 with the DHT method.

XPS was also used to identify the oxidation state of Mn in the DHT and TIE samples. The binding energies of Mn $2p_{3/2}$ for both TIE and DHT samples were located around 641.4 eV, coinciding with the binding energies of MnO (640.5–641.4 eV) and Mn_3O_4 (641.4 eV) [34,35]. Such results agreed with the conclusion obtained by ESR, EXAFS and UV–VIS studies that Mn^{2+} and Mn^{3+} coexisted in the Mn-MCM-41 prepared by either DHT or TIE method.

3.3. Epoxidation of styrene over Mn-MCM-41 synthesized by DHT and TIE methods

The effects of solvents and oxidants on the epoxidation of styrene over the Mn-MCM-41 prepared by the DHT method were first examined and the results are shown in Table 4. In all the cases, styrene oxide and benzaldehyde were mainly produced. When MeOH was used as the solvent, styrene oxide produced further reacted with methanol to form methoxyphenylacetic acid in a selectivity of 40% (Table 4, run 4). A small amount of phenylacetaldehyde (abbreviated as PhAcH in Table 4, run 3) was also formed when MeCN was used. The highest styrene conversion was achieved by using MeCN. The selectivity to styrene oxide could be improved when a small amount of DMF was added to MeCN as reported previously during the epoxidation of stilbene over a Mn-MCM-41 prepared by the TIE method [17]. We used the mixture of DMF and MeCN as the solvent in most of our studies.

H_2O_2 and iodosobenzene (PhIO) were also examined as oxidant. With 30% H_2O_2 aqueous solution, the rapid decomposition of H_2O_2 occurred and no oxidation product was obtained except for a very small amount of benzaldehyde (Table 4, run 5). PhIO as the oxidant exhibited both lower styrene conversion and poorer selectivity to styrene oxide as compared with TBHP as the oxidant (Table 4, run 6).

Table 5 compares the catalytic properties of the Mn-MCM-41 synthesized by both DHT and TIE

Table 4
Effect of solvents and oxidants on the epoxidation of styrene[a]

Run	Solvent (ml)	Oxidant (mmol)	Styrene conversion (%)	Selectivity (%)			Sty.oxide yield (%)
				Sty.oxide	Benzald.	PhAcH	
1	DMF (10)	TBHP (10)	3.2	62.5	37.5	0.0	2.0
2	DMF + MeCN (1 + 9)	TBHP (10)	10.9	70.3	27.2	2.5	7.7
3	MeCN (10)	TBHP (10)	13.4	64.6	27.8	6.6	8.8
4[b]	MeOH (10)	TBHP (10)	4.8	20.0	40.0	0.0	1.0
5[c]	DMF + MeCN (1 + 9)	H_2O_2 (9.79)	0.4	0.0	100.0	0.0	0.0
6[d]	MeCN (10)	PhIO (5)	3.3	25.7	74.3	0.0	0.9

[a] Catalyst: Mn-MCM-4-DHT (Si/Mn = 211), 0.2 g; $T = 60\,^{\circ}C$; $t = 24$ h; styrene, 10 mmol.
[b] The other product: methoxyphenylacetic acid.
[c] $t = 2.8$ h.
[d] Catalyst: Mn-MCM-41-DHT (Si/Mn = 47), 0.2 g; styrene, 5 mmol; PhIO, 5 mmol.

methods with different Si/Mn ratios for the epoxidation of styrene. For both types of catalysts, the conversion of styrene increased with an increase in Mn content, supporting that Mn was the active site for epoxidation reactions. The styrene conversion over the TIE catalyst was about twice as high as that over the DHT catalyst with the same Mn content. As described above, most of the manganese sites were probably dispersed on the surface of mesoporous channels in the TIE samples, while some manganese atoms were incorporated inside the wall of MCM-41 in the DHT samples. It is likely that the Mn sites on the surface of mesoporous channels are more active than those incorporated inside the framework. Benzoic acid and mandelic acid were also produced probably from the consecutive oxidation of benzaldehyde and styrene oxide, respectively over the TIE samples. However, the efficiency of TBHP for the conversion of styrene is remarkably higher over the DHT samples.

3.4. Epoxidation of trans-stilbene and cis-stilbene

Iwamoto and coworkers [17] reported the epoxidation of both *trans*-stilbene and *cis*-stilbene over Mn-MCM-41 synthesized by the TIE method. They, however, used oxidant (TBHP) in a large excess amount (mol ratio of TBHP/stilbene = 14) and did not mention about the efficiency of TBHP [17]. We think that the efficiency of TBHP is also a vital standard for evaluating a catalyst. Table 6 compares the catalytic properties of the DHT and TIE samples in the epoxidation of *trans*-stilbene and *cis*-stilbene. In a similar way to that observed for styrene oxidation, the TIE sample with a Mn content of 1.48 wt.% (Si/Mn = 61) exhibited higher conversion of stilbene

Table 5
Comparison of catalytic properties of Mn-MCM-41 prepared by the DHT and TIE methods for epoxidation of styrene[a]

Catalyst (Si/Mn)	Styrene conversion (%)	Selectivity (%)			Sty.oxide yield (%)	TBHP conversion (%)	TBHP efficiency (total, %)	TBHP efficiency (oxide, %)
		Sty.oxide	Benzald.	Others[b]				
Mn-MCM41(359), DHT	10.1	76.8	23.2	0.0	7.8	10.7	95.2	72.9
Mn-MCM41(211), DHT	10.9	70.3	27.2	2.5	7.7	13.6	79.8	56.6
Mn-MCM41(91), DHT	15.8	79.8	20.2	0.0	12.6	16.8	93.6	74.9
Mn-MCM41(47), DHT	17.9	81.9	18.1	0.0	14.7	18.0	99.4	81.7
Mn-MCM41(124), TIE	28.8	74.6	16.1	9.3	21.5	49.5	58.2	43.4
Mn-MCM41(61), TIE	32.8	73.2	15.9	10.9	24.0	52.5	62.5	45.7
Mn-MCM41(33), TIE	39.8	69.4	14.5	16.1	27.6	59.1	67.3	46.7

[a] Catalyst, 0.2 g; $T = 60\,^{\circ}C$; $t = 24$ h; solvent, DMF (1 ml) + MeCN (9 ml); styrene, 10 mmol; TBHP, 10 mmol.
[b] The total selectivity to benzoic acid, mandelic acid and phenylacetaldehyde.

Table 6
Epoxidation of *trans*-stilbene and *cis*-stilbene over Mn-MCM-41 prepared by the DHT and TIE methods[a]

Catalyst (Si/Mn)	Synthesis method	Configuration	Stilbene conversion (%)	Selectivity (%)				*trans*-Stilbene oxide yield (%)	TBHP conversion (%)	TBHP efficiency (%)
				trans-Stilbene	*cis*-Stilbene	Benzald.	Benz. acid			
MnMCM-41(47)	DHT	*trans*	41.5	85.5	0.0	14.5	0.0	35.5	6.9	59.4
MnMCM-41(61)	TIE	*trans*	56.5	93.5	0.0	6.0	0.5	52.9	37.3	15.1
MnMCM-41(47)[b]	DHT	*trans*	74.0	87.7	0.0	4.1	8.1	64.9	35.8	20.7
MnMCM-41(61)[b]	TIE	*trans*	81.7	81.4	0.0	4.1	14.8	67.0	57.8	14.1
MnMCM-41(47)	DHT	*cis*	16.0	88.8	0.0	11.2	0.0	14.2	14.4	11.1
MnMCM-41(124)	TIE	*cis*	20.0	88.4	1.0	11.7	0.0	17.7	27.9	7.2

[a] Catalyst, 0.2 g; $T = 60\,^{\circ}C$; $t = 24$ h; stilbene, 1 mmol; solvent: MeCN(9 ml) + DMF(1 ml); TBHP, 10 mmol.
[b] $t = 72$ h.

than the DHT sample with a Mn content of 1.91 wt.% (Si/Mn = 47), while the product distributions were similar, i.e. *trans*-stilbene oxide and benzaldehyde were mainly obtained. However, higher efficiency of TBHP was obtained over the DHT sample. For a 24 h reaction, the conversion of TBHP on the TIE samples was 5.4 times as high as (Table 6, runs 1 and 2) that on the DHT sample, resulting in a very low TBHP efficiency of the TIE sample (15.1%) than that of the DHT sample (59.4%).

For the oxidation of *cis*-stilbene, in addition to benzaldehyde, only *trans*-stilbene oxide was produced over both DHT and TIE samples. This feature resembles that reported by Iwamoto and coworkers [17] in the epoxidation of *cis*-stilbene over the TIE catalyst. Thus, irrespective of the synthetic methods, it is likely that the epoxidation reactions with TBHP over the Mn-MCM-41 proceed through a radical intermediate. As shown in Table 6, the conversion of *cis*-stilbene was much lower than that of *trans*-stilbene over the same catalyst. The lower reactivity of *cis*-stilbene may be due to the steric hindrance that retards the reaction between substrate and oxygen species.

4. Conclusions

Mn-MCM-41 was found to be the most effective catalyst for the epoxidation of styrene using TBPH as an oxidant among Mn-, V-, Cr-, Fe- and Mo-containing MCM-41. As suggested by the characterizations with ESR, XANES, UV–VIS and UV–Raman, both Mn^{2+} and Mn^{3+} coexisted on the Mn-MCM-41 synthesized by both DHT and TIE methods, and some Mn cations might be incorporated into the framework of MCM-41 in the DHT samples. The epoxidation of both styrene and stilbene using TBHP as the oxidant afforded the corresponding epoxides. The TIE sample exhibited higher conversion of styrene and stilbene than the DHT sample with the same Mn content, but the DHT sample afforded higher TBHP efficiency.

Acknowledgements

The X-ray absorption experiments were performed under the approval of the Photon Factory Program Advisory Committee (Proposal 2002G097).

References

[1] A. Corma, Chem. Rev. 97 (1997) 2373.
[2] J.M. Thomas, Angew. Chem., Int. Ed. Engl. 38 (1999) 3588.
[3] H. Berndt, A. Martin, A. Bruckner, E. Schreier, D. Muller, H. Kosslick, G.-U. Wolf, B. Lucke, J. Catal. 191 (2000) 384.
[4] J.M. Thomas, T. Maschmeyer, B.F.G. Johnson, D.S. Shephard, J. Mol. Catal. A 141 (1999) 139.
[5] M. Morey, A. Davidson, H. Eckert, G. Stucky, Chem. Mater. 8 (1996) 486.
[6] P. Sutra, D. Brunel, J. Chem. Soc., Chem. Commun. (1996) 2485.
[7] M. Yonemitsu, Y. Tanaka, M. Iwamoto, Chem. Mater. 9 (1997) 2679.
[8] R.D. Oldroyd, J.M. Thomas, T. Maschmeyer, P.A. MacFaul, D.W. Snelgrove, K.U. Ingold, D.D.M. Wayner, Angew. Chem., Int. Ed. Engl. 35 (1996) 2787.
[9] Q. Zhang, Y. Wang, Y. Ohishi, T. Shishido, K. Takehira, Chem. Lett. (2001) 194.
[10] Y. Wang, Q. Zhang, Y. Ohishi, T. Shishido, K. Takehira, Catal. Lett. 72 (2001) 215.
[11] Q. Zhang, Y. Wang, Y. Ohishi, T. Shishido, K. Takehira, J. Catal. 202 (2001) 308.
[12] Q. Zhang, Y. Wang, S. Itsuki, T. Shishido, K. Takehira, Chem. Lett. (2001) 946.
[13] T. Katsuki, J. Mol. Catal. A: Chem. 113 (1996) 87.
[14] S.-S. Kim, W. Zhang, T.J. Pinnavaia, Catal. Lett. 43 (1997) 149.
[15] V. Caps, S.C. Tsang, Catal. Today 61 (2000) 19.
[16] R. Burch, N. Cruise, D. Gleeson, S.C. Tsang, J. Chem. Soc., Chem. Commun. (1996) 951.
[17] M. Yonemitsu, Y. Tanaka, M. Iwamoto, J. Catal. 178 (1998) 207.
[18] D. Dollimore, G.R. Heal, J. Appl. Chem. 14 (1964) 109.
[19] Z. Luan, J. Xu, H. He, J. Klinoswki, L. Kevan, J. Phys. Chem. 100 (1996) 19595.
[20] J. Xu, A. Luan, T. Wasowicz, L. Kevan, Micorpor. Mesopor. Mater. 22 (1998) 179.
[21] Z. Levi, A.M. Raitsimring, D. Goldfarb, J. Phys. Chem. 95 (1991) 7830.
[22] J.C. Vedrine, in: F. Delannay (Ed.), Characterization of Heterogeneous Catalysis, Marcel Dekker, New York, 1984, p. 161.
[23] D. Zhao, D. Goldfarb, J. Chem. Soc., Chem. Commun. (1995) 875.
[24] N.M.D. Brown, J.B. McMonagle, J. Chem. Soc., Faraday Trans. 1 80 (1984) 589–597.
[25] M.Y. Apte, C. Mande, J. Phys. C: Solid State Phys. 15 (1982) 607–613.
[26] S.I. Salem, C.N. Chang, P.L. Lee, V. Severson, J. Phys. C: Solid State Phys. 11 (1978) 4085–4093.
[27] S. Velu, N. Shah, T.M. Jyothi, S. Sivasanker, Micropor. Mesopor. Mater. 33 (1999) 61.
[28] F. Milella, J.M. Gallardo-Amores, M. Baldi, G. Busca, J. Mater. Chem. 8 (1998) 2525.
[29] C. Li, G. Xiong, Q. Xin, J. Liu, P. Ying, Z. Feng, J. Li, W. Yang, Y. Wang, G. Wang, X. Liu, M. Lin, X. Wang, E. Min, Angew. Chem., Int. Ed. Engl. 38 (1999) 2220.

[30] G. Xiong, C. Li, H. Li, Q. Xin, Z. Feng, Chem. Commun. (2000) 677.
[31] G. Ricchiardi, A. Damin, S. Bordiga, C. Lamberti, G. Spano, F. Rivetti, A. Zecchina, J. Am. Chem. Soc. 123 (2001) 11409.
[32] J. Yu, Z. Feng, L. Xu, M. Li, Q. Xin, Z. Liu, C. Li, Chem. Mater. 13 (2001) 994.
[33] F. Buciuman, F. Patcas, R. Cracium, D.R.T. Zahn, Phys. Chem., Chem. Phys. 1 (1999) 185.
[34] F. Mirabella, J. Ghijsen, R.L. Johnson, Z. Golacki, B.A. Orlowski, J. Alloys Comp. 328 (2001) 166–170.
[35] X-Ray Photoelectron Spectroscopy, Surf. Sci. Soc. Jpn. Maruzenn, Tokyo, 1998.